Chapter 4:

Effect of Metallic Impurities on Photoconductivity of Se-Te Based Chalcogenide Thin films

Photoconductivity is an optical and electrical phenomenon in which a material becomes more electrically conductive due to the absorption of illuminating light, especially in the visible region. It is different from conductivity induced by the bombardment of particles or laser irradiation. The phenomenon of photoconductivity was observed by Willoughby Smith in 1873 with a selenium resistor [1]. Subsequently widespread research had been carried out on different materials to understand this phenomenon and use it for various applications. As a result many of the photoconductors found applications in various systems. Although all insulators and semiconductors can said to be photoconductive as they show some increase in electrical conductivity when illuminated by light of sufficiently high energy to create free carriers but the number of materials for which the increase in conductivity is large enough to be useful is fairly limited. Only a few materials show a large enough photosensitivity to be practically useful in applications of photoconductors. The reason for this is that many of the characteristics of a material which determine its sensitivity to light are associated with imperfections in their structure. Only in certain materials these imperfections are of such a nature as to permit the long lifetimes of the excited charge carriers necessary to produce a large increase in conductivity. Photoconductivity serves as a tool to understand the internal processes in these materials, and it is widely used to detect the presence of light and measure its intensity in light-sensitive devices. Different models were suggested for the characteristics of photoconductivity in materials [2-5].

Photoconductive materials are used in the manufacture of photoelectric devices. Typical photoconductive substances consist of germanium, gallium, selenium, or silicon with added impurities, also known as *dopants or additives*. Photoconductivity ensues when the material is illuminated with photons of sufficient energy to raise charge carriers across the band gap. Because the current ceases when the light is removed, photoconductive materials form the basis of light-controlled electrical switches. These materials are also used to detect infrared radiation in military applications such as guiding missiles to heat-producing targets. Photoconductivity has broad commercial application in the process of photocopying, or xerography, which originally used selenium but now relies on photoconductive polymers. Most semiconductor materials have this property. When light is absorbed by such a semiconductor, the number of free electrons and holes changes and raises its electrical conductivity.

ISBN: 978-81-936820-2-9
Thesis DOI: 10.21467/thesis.2

Series: AIJR Thesis

4.1 Photoconductivity in Chalcogenide Glasses

Photoconductivity is the improved electrical conductivity of matter produced by the motion of carriers created by absorbed light. In the dark, under conditions of thermal equilibrium, the thermally generated carriers are distributed among the available energy states in accordance with Fermi-Dirac Statistics. These electrons and holes occupying conduction bands determine the dark electrical conductivity of the material. Under illumination, a steady state is reached in which the rate of photo-generation is balanced by the various recombination processes, through which the carriers tend to relax to the normal equilibrium distribution. The phenomenon thus involves absorption, photo-generation, recombination and transport processes and an intimate relationship exist between them. This is one reason for the critical role played by photoconductivity in the development and understanding of the physics of semiconductors. The compositional disorder introduces large densities of states within the band gap. These can limit carrier lifetime and thus photosensitivity. In some materials considerable fluctuation in observed properties can occur depending on the preparation conditions.

The excess conductivity due to absorbed light is given by [6-10]

$$\Delta\sigma = e(\Delta n\mu_n + \Delta P\,\mu_p) \qquad (4.1)$$

μ represents mobility of the corresponding carriers. The increase in conductivity is due to the increase in the densities of n and p charge carriers due to light illumination. Under steady state conditions, the excess densities are equal to their rate of generation g which is the number of carriers generated per unit time in unit volume multiplied by their average lifetime τ

$$\Delta n = g\,\tau_n \text{ and } \Delta p = g\tau_p \qquad (4.2)$$

The generation rate is governed by the quantum yield η, which is the number of electron-hole pairs generated by the absorption of a photon. The non-equilibrium charge carriers exist until they disappear by recombination of a free electron with a free hole, capture of an electron by a centre in which a hole is localized and capture of a hole by a centre in which there is a bound electron. In steady state the rates of generation and recombination of carriers are equal.

The band structure of amorphous semiconductor exhibits discrete energy levels associated with defect states as mentioned in chapter1. Different approaches have been adopted regarding the band structure of photoconductors [11, 12].

The common factor in chalcogen elements is the presence of six electrons in their outer valence shell. When neutral, the atoms have two electrons paired in a filled s shell, two more in a filled p shell, and one each in the other two p shells. This configuration leaves two unfilled states in p orbital to participate in the formation of chemical bonds. Thus, these atoms tend to form structures in which the chalcogen atom has two covalent chemical bonds. For a variety of chalcogenide, several estimation of ionicity of the bonds suggests that they are more than 80% covalent compounds [13]. All of the chalcogenide-rich glasses appear to share a common

electronic band structure. The chalcogen atoms all have six valence electrons in an s^2p^4 configuration. As mentioned earlier, the s shell and one p shell are completely full. The full p shell is known as a lone-pair (LP) orbital. The other two half-filled p shells participate in the formation of covalent bonds, so the chalcogen atoms are normally two fold coordinated. The valence band of chalcogenide glasses consists of state from the p bonding (σ) and LP orbitals. The LP electrons have higher energy than the bonding electrons, so the full LP band forms the top of the valence band. The conduction band is formed by the antibonding (σ*) band. The LP band falls between the σ and σ* bands, so the bandgap is about half of the bonding-anti bonding splitting energy [14, 15]. Because the electrical properties are determined by the LP band, these materials are called lone-pair semiconductors [12]. An example of the band structure based on Kastner [14] has been shown in figure 4.1 below.

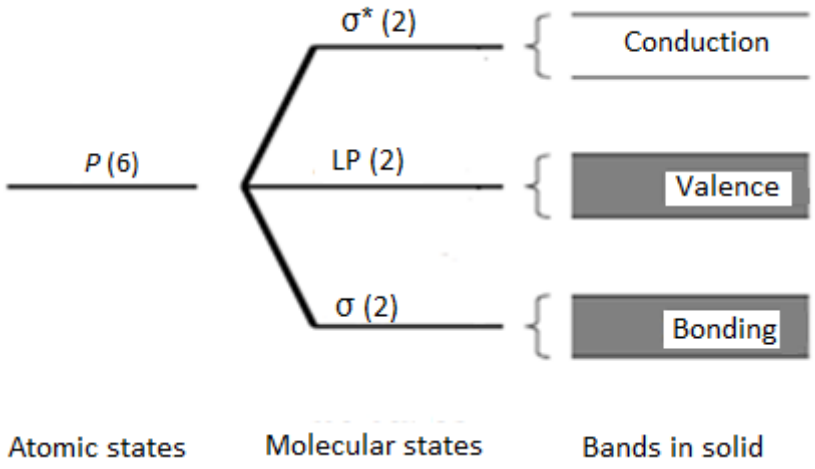

Figure 4.1: Band structure of lone-pair semiconductors [14].

Optical excitations of band edge electrons involve excitation of the lone-pair electrons into the conduction band. Even in alloys, the optical behavior of the glass is strongly determined by the nature and environment of the lone-pair electrons. One of the most interesting optical properties of the chalcogenide glasses is their inherent photosensitivity. The photosensitivity is only observed when samples are in the amorphous state [11, 12] and is strongly influenced by the type of chalcogen atom and the nature of the LP band. Electronically, the chalcogenide glasses behave as semiconductors. They have a band gap, and consequently they are transparent to a certain range of wavelengths of light. The disorder of the network creates localized electronic states that extend into the forbidden band gap. These states have a significant effect on the electrical and optical properties of the chalcogenide glasses. The transparent window extends far into the infrared because the infrared side of the transparent region is determined by the phonon energy of the material. The photo induced effect can

occur by illuminating with light, so long as the light has sufficient energy to excite electrons from the LP band [14].

Compositions containing tellurium tend to have the smallest band gap [15] and the highest conductivity, the conductivity comes from the disorder of the amorphous structure. The intrinsic disorder in an amorphous material creates localized electronic states near the band edges [16, 17]. These cause low carrier mobility because they act as traps and scattering centers for conduction band electrons and valence band holes. The conduction mechanism is not well known and several models have been proposed such as the Davis-Mott model and the small-polaron model [17]. In the Davis-Mott model, conduction occurs by one of three possible paths depending on the temperature. At low temperatures, conduction occurs by electron hopping between mid-gap localized states. Conduction by electrons excited into localized states at the band edges occurs at higher temperatures. At even higher temperatures, electrons can be directly excited to extended states. In the small polaron model, the charge carriers are small-polarons and conduction occurs by thermally activated hopping. The small-polaron model is the generally accepted model for electronic conduction in glasses.

4.2 Experimental Procedure

Steady state and transient Photoconductivity measurements have been carried out in Se-Te-Al and Se-Te-Hg glassy alloys. Involved experimental procedure for the photoconductivity measurements of thin films are described in the following paragraphs.

4.3 Preparation of Thin Film with Electrode

The glassy alloys of the sample have been prepared by melt quenching technique as describe in section 3.2.1. For electrical contacts, Indium electrode has been deposited on pre-cleaned glass substrate by thermal evaporation technique. Pure Indium metal has been taken for evaporation. Thin film of prepared alloy having thickness of 300 nm deposited on Pre-deposited Indium electrodes on glass substrate by thermal evaporation technique as describe in section 3.2.2. The dark and photoconductivity measurements of the amorphous films have been studied at 298-373 K by mounting it in a specially designed metallic sample holder as describe in next section.

4.4 Dark Conductivity and Photo Conductivity Measurement

Conductivity measurement has been done by standard and most common two-probe method. For dc conductivity measurement in thin films metallic sample holders are designed in the lab as shown in figure 4.2. The probes were mounted on a suitable stand which also holds the sample plate, heater and thermocouple. Two copper probes for electrical contact have been mounted on a metallic plate separated by Teflon bolts. Area of contact of the probes on the sample should be small compared to the distance between the contacts. The voltage and current leads were taken out using insulated wires. A heater of 25 W has been fitted backside

the plate on which the sample to be mounted. The heater power supply has been provided from a variac. A chromel-alumel thermocouple has been fitted near the sample to read the sample temperature. The sample holder has been placed in a metallic chamber under vacuum of 10^{-3} Torr to avoid atmospheric reaction during heating. This chamber contains a transparent window on the same level of thin film holder. Through this window light can be shine on to the sample for illumination.

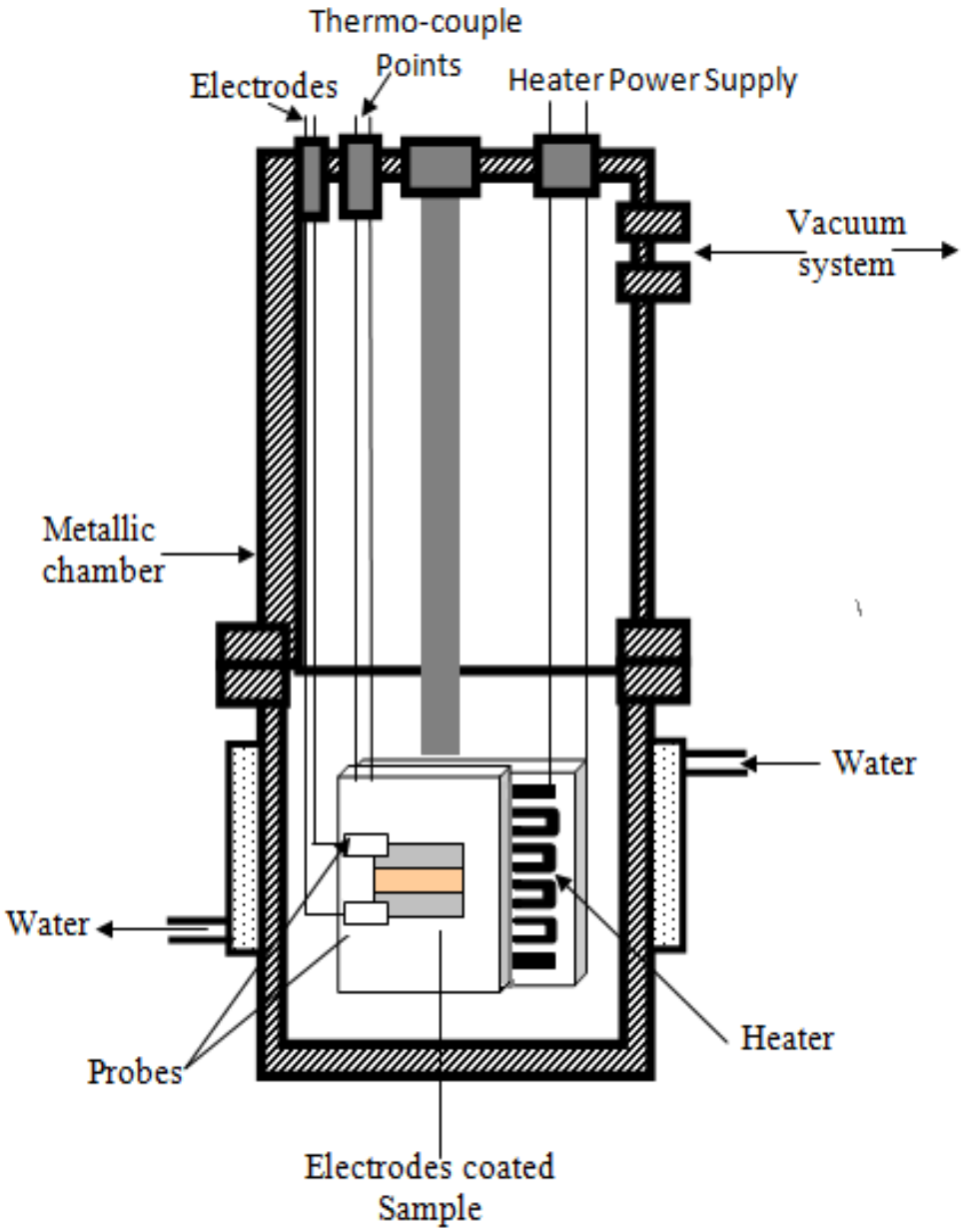

Figure 4.2: Sample holder for dc-conductivity measurements on thin films

For d.c. conductivity measurement thin film with indium electrode has been mounted in thin film holder. D. C. voltage has been applied across the sample using power supply (ScienTECH ST4073). The current has been measured using a picoammeter (Keithley 6485). The temperatures were slowly increased with the help of variac and the resulting current has been measured with picoammeter.

Photoconductivity measurement has been done in same sample holder. Layout of measurement setup has been shown in figure 4.3. Thin film with electrode has been mounted in thin film holder and white light using 200W tungsten lamp has been shine through transparent window. The intensity of light has been measured by a digital Lux-meter (MS6610).

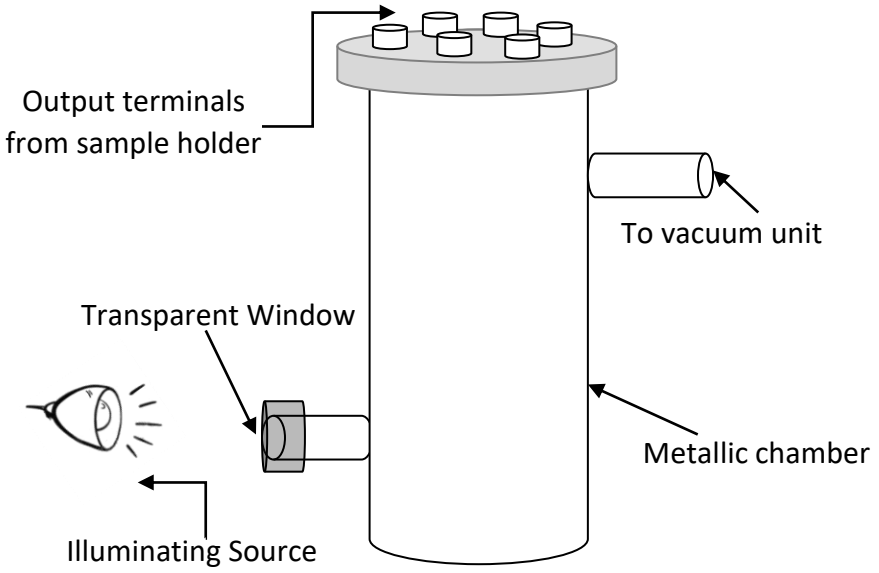

Figure 4.3: Layout of photoconductivity measurement setup

For the transient photoconductivity measurement, light has been shined on sample and photocurrent of corresponding time has been noted. When saturation was reached, the light was turned off and the decay in the current has been noted with time.

The dark current (I_{dc}) and photocurrent under iIlumination (I_{ill}) has been measured. The photocurrent (I_{ph}) is calculated using relation [18, 19]-

$$I_{ph} = I_{ill} - I_{dc} \quad (4.3)$$

The conductivity of specimen is given by the equation

$$\sigma = IL/VA \quad (4.4)$$

where, I is the current measured in ampere, the voltage in volts, A is the cross sectional area in cm^2 and L is the length of the sample in cm.

4.5 Study of Photo-induced Effect

Photoconductivity is an intrinsic property of the chalcogenide glasses. It leads to a variety of interesting effects, which as a group can be labeled photo-induced effect and make structural changes. The changes in structure are caused by the absorption of above or below band gap light and the subsequent relaxation of the excited state into a new metastable structure. The ability to control the structure and properties of the chalcogenide glasses with light makes them uniquely suitable for applications in optics and microfabrication. In this chapter photo induced effect on $Se_{88}Te_{12-x}Al_x$ and $Se_{96-x}Te_4Hg_x$ thin films have been studied and explained.

4.6 Photoinduced Effect on $Se_{88}Te_{12-x}Al_x$ Thin Films.

The temperature dependence of the dark current and the photocurrent have been studied in glassy $Se_{88}Te_{12-x}Al_x$ (X = 4, 6, 8 and 10) thin films in the temperature range 298 K- 373 K. The conductivity has been measured as a function of temperature at a constant voltage of 3V for all samples using equation 4.4. Taking results of these measurements $\ln(\sigma_{dc})$ versus 1000/T have been plotted and shown in Figure 4.4. Plot of temperature dependence of dark conductivity $\ln(\sigma_{dc})$ for $Se_{88}Te_{12-x}Al_x$ thin films found almost linear, indicating that the conduction is through an activated process having single activation energy. Therefore, σ_{dc} can be expressed by Arrhenius relation-

$$\sigma_{dc} = \sigma_o \exp(-\Delta E_{dc}/kT) \qquad (4.5)$$

where, σ_0 is the material related pre-exponential factor, ΔE_{dc} is the activation energy for dc conduction, k is the Boltzman constant and T is the absolute temperature. The value of ΔE_{dc} is estimated from the slope of $\ln(\sigma_{dc})$ versus 1000/T curves. The calculated value of σ_{dc} , ΔE_{dc} and σ_0 at room temperature is given in table 4.1.

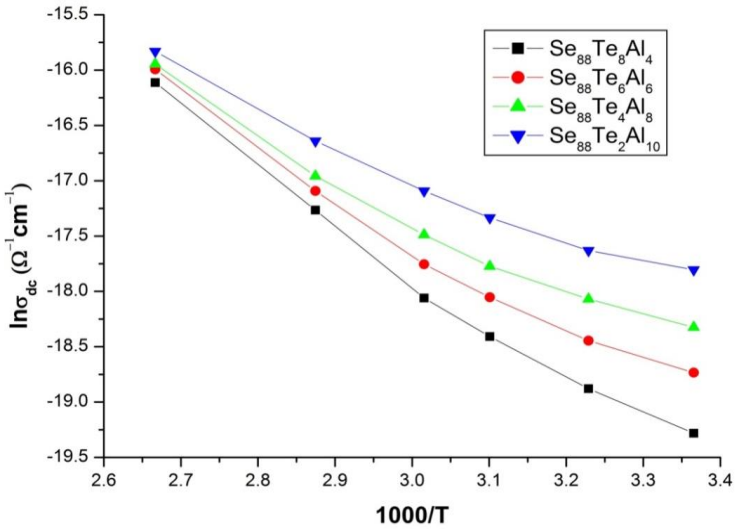

Figure 4.4: Temperature dependence of dark conductivity for various samples in a - $Se_{88}Te_{12-x}Al_x$ thin films.

From result it is observed that σ_{dc} increases with Al concentration in $Se_{88}Te_{12-x}Al_x$ glassy alloy. ΔE_{dc} and σ_0 found to be decrease with Al concentration. The addition of more metallic impurities, in general, is expected to lower the activation energy [20, 21].

Temperature dependence of steady state photoconductivity has been studied in $Se_{88}Te_{12-x}Al_x$ system. It is found that $\sigma_{ph} > \sigma_{dc}$ in all sample and σ_{ph} also increases with Al content. $\ln\sigma_{ph}$ versus 1000/T has been plotted and shown in figure 4.5, which shows linear curve indicating that the photoconductivity is an activated process. The activation energy for photoconduction (ΔE_{ph}) is calculated from the slopes of $\ln\sigma_{ph}$ versus 1000/T curves and the values are given in table 4.1. The activation energy of photoconduction is much smaller than the activation energy in the dark. The well-defined activation energies involved in the temperature dependence of photoconductivity suggests that the recombination centres are located at relatively discrete levels of localized states [21]. It is observed that ΔE_{ph} also decreases with increase in Al content.

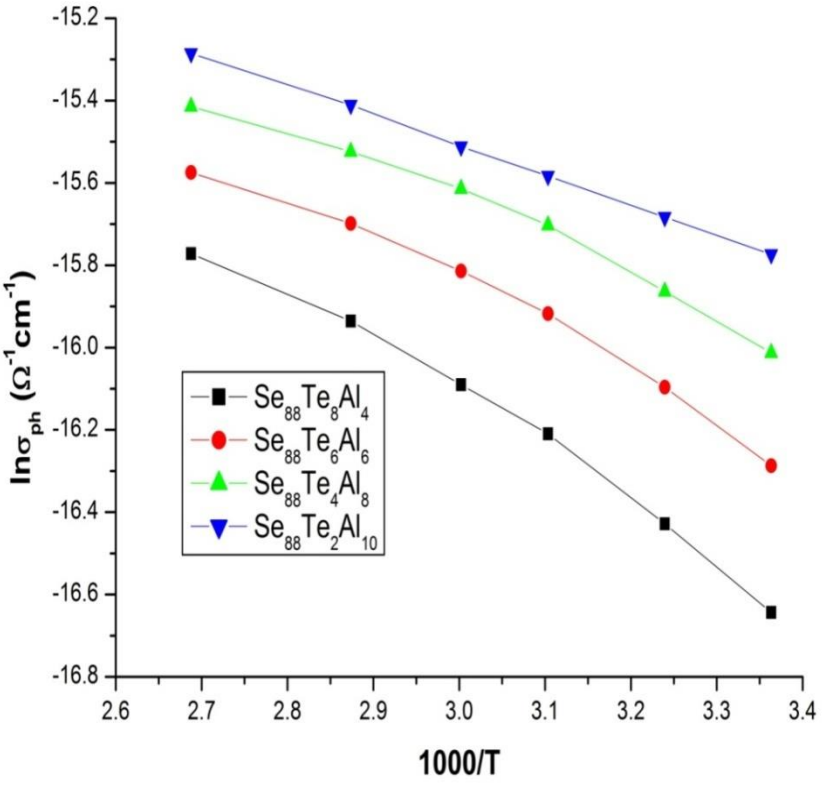

Figure 4.5: Temperature dependence of photoconductivity for various samples in a - $Se_{88}Te_{12-x}Al_x$ thin films

Table 4.1: Various conductivity parameters at room temperature

Sample / Parameter	$Se_{88}Te_8Al_4$	$Se_{88}Te_6Al_6$	$Se_{88}Te_4Al_8$	$Se_{88}Te_2Al_{10}$
σ_{dc} ($\Omega^{-1}cm^{-1}$)	4.42 X 10^{-9}	8.89 X 10^{-9}	1.43 X 10^{-8}	2.99 X 10^{-8}
ΔE_{dc} (eV)	0.39	0.34	0.29	0.24
σ_0 ($\Omega^{-1}cm^{-1}$)	1.72 X 10^{-2}	3.50 X 10^{-3}	8.49 X 10^{-4}	2.36 X 10^{-4}
σ_{ph} ($\Omega^{-1}cm^{-1}$)	5.51 X 10^{-8}	8.44 X 10^{-8}	1.11 X 10^{-7}	1.41 X 10^{-7}
ΔE_{ph} (eV)	0.11	0.09	0.08	0.06
σ_{ph}/σ_{dc}	12.58	9.55	7.86	4.86
γ	0.66	0.62	0.63	0.64
PPC	0.040	0.043	0.048	0.052
τ_d (S)	4.44	4.50	4.52	10.35
τ_c (S)	0.23	0.24	0.29	0.34

Steady state photoconductivity measurements as a function of light intensity (F) were also performed on the a- $Se_{88}Te_{12-x}Al_x$ thin films at room temperature (298 K). The results of these measurements are shown in figure 4.6.

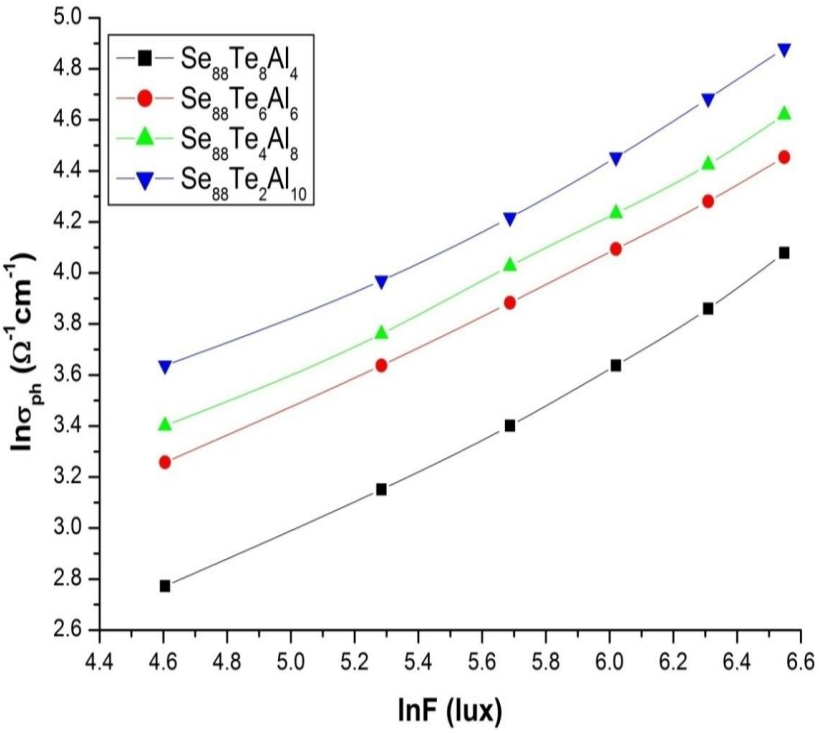

Figure 4.6: Variation of photoconductivity as a function of light intensity in a - $Se_{88}Te_{12-x}Al_x$ thin films

It is clear from this figure that, $\ln\sigma_{ph}$ versus lnF curves are nearly straight lines which indicate that photoconductivity follows a power law with intensity [22, 23]

$$\sigma_{ph} \quad \alpha \quad F^{\gamma} \qquad (4.6)$$

In the system studied, the power γ has been calculated from the slopes of $\ln\sigma_{ph}$ versus lnF curves and given in table 4.1. It is found that γ varies from 0.62 to 0.66 for different compositions indicating the presence of localized or traps states in the gap of the material [22]. For a given material, the photosensitivity (σ_{ph}/σ_{dc}) is an important parameter to decide its use in photoconductive applications. σ_{ph}/σ_{dc} values for different compositions have been calculated at 600 lux at room temperature and given in Table 4.1. It is observed that photosensitivity decreases with increasing Al %.

Transient photoconductivity measurements have been taken by illuminating the light of intensity 600 lux at temperature 298 K on the sample. After turning on light rise in current with time has been noted. After a certain time of illumination, when steady state achieved, light has been turned off and decay of the photocurrent has been measured. The initial dark current has been subtracted to obtain transient photocurrent. The rise and decay of photocurrent with time for all compositions are shown in Figure 4.7.

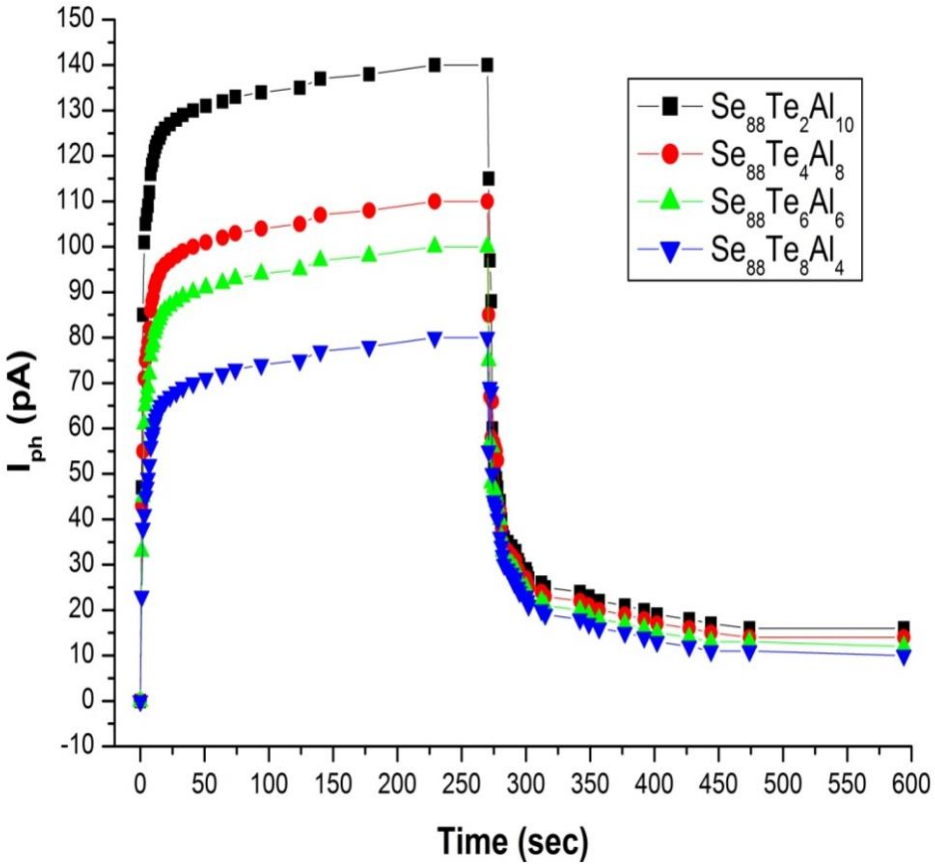

Figure 4.7: The rise and decay of photocurrent with time for all compositions

It is clear from Figure 4.7 that the photocurrent initially rises fast then becomes slows, saturating after certain time. After get saturation current the light has been switched off and the photocurrent starts to decay quite fast initially, and then becomes slow. As time elapses it reaches steady state value as shown in figure 4.7. The decay process seems to be composed of two processes, a faster decay at the onset of transient and a slower decay later on. A persistent photocurrent is observed in all compositions of $Se_{88}Te_{12-x}Al_x$, which does not decay even after a long time interval. Such long-lived photocurrent has also been observed in other chalcogenide glasses [24-41]. It is believed that such a large decay constant can not be due to carriers trapped in the intrinsic defects [42]. It may be due to defects produce in structure on increasing Al content. To compare the persistent photocurrent effect with Al content, we calculate the quantity Persistent Photoconductivity (PPC) [43, 44] as-

$$PPC = (\sigma_l - \sigma_{dc}) / \sigma_{dc} \quad (4.7)$$

where σ_l the total photo conductivity of the light induced state after the decay of 350 seconds, and σ_{dc} is the dark conductivity of the amorphous state. $(\sigma_l - \sigma_{dc})$ represent the persistence photoconductivity. It is found that PPC increases with Al content. The persistent photocurrent is subtracted from the measured photocurrent and then the corrected photocurrent has been used for further analysis. Corrected decay photocurrent has been plotted against time (t) for all compositions as shown in figure 4.8.

The decay of photocurrent strongly depends upon the characteristics of traps in a given material. For analysis of decay rates in the case of non-exponential decay, differential lifetime (τ_d) has been calculated using the Fuhs and Meyer [45] relation -

$$\tau_d = -\left[\frac{1}{I_{ph}}\left(\frac{dI_{ph}}{dt}\right)\right]^{-1} \quad (4.8)$$

In the case of non-exponential decay, differential lifetime (τ_d) is time dependent. From the slope of corrected I_{ph} versus time the values of differential lifetime has been calculated using the equation 4.8. The value of the differential lifetime at t = 8s has been chosen to compare the rate of decay of all compositions and given in table 4.1. Differential lifetime increases slightly with increase in Al concentration but at higher concentration of Al differential lifetime increases drastically. Higher the value of differential lifetime after the Al addition shows the slower rate of decay of photocurrent. For exponential decay, the differential life time will be equal to the carrier life time (τ_C). It is found that at a particular time carrier life time increase with Al content and calculated value of carrier lifetime is given in table 4.1.

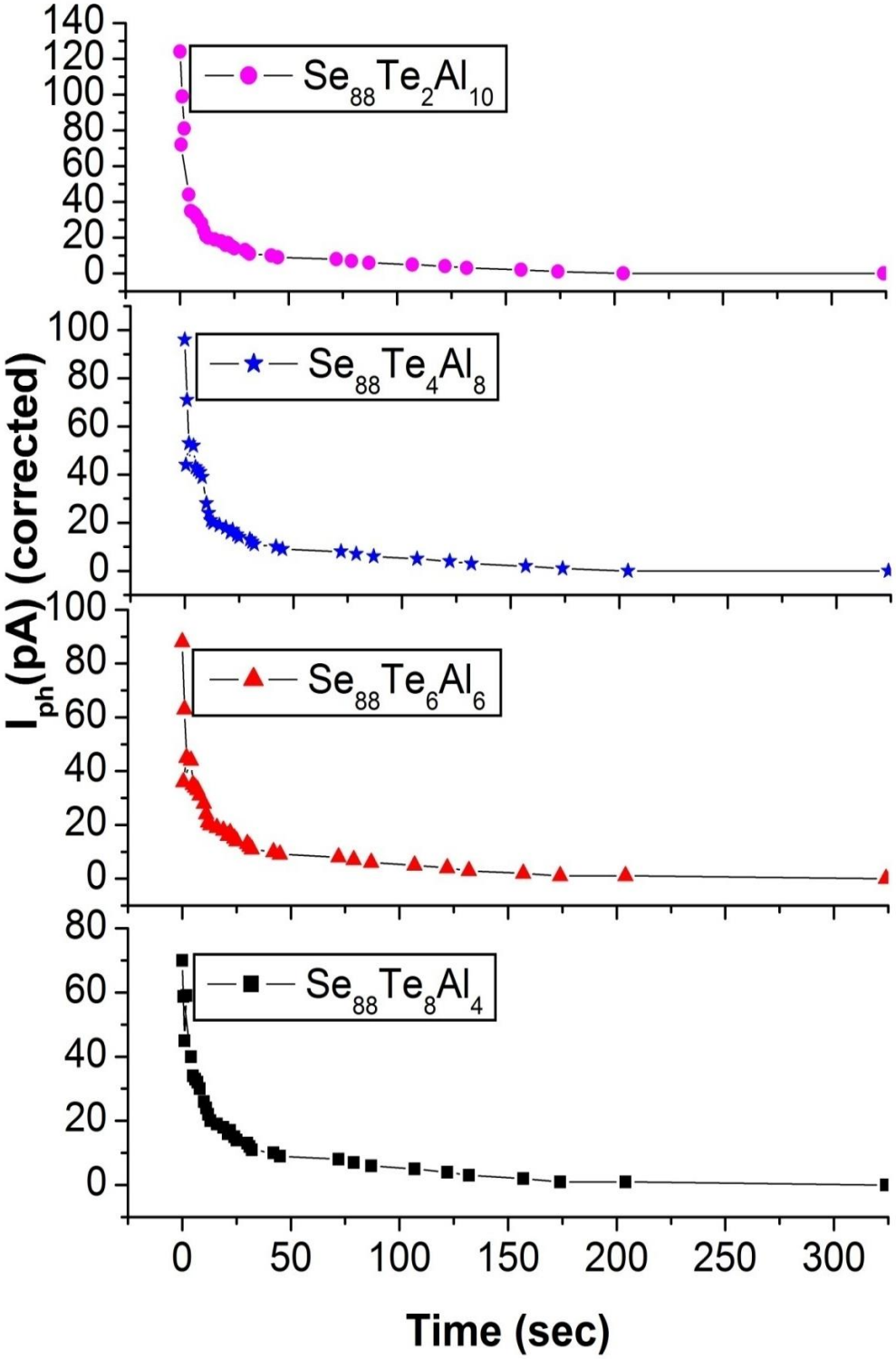

Figure 4.8: Variation of corrected photocurrent for decay against time (t) for all compositions.

Conductivity measurement show that electrical dark conductivity and photo conductivity increased with higher doping concentration of Al. The electrical photo conductivity is higher than dark conductivity. This relation is inversely proportional to current resistivity [46, 47]. From I-V graph shown in figure 4.9, the resistivity at every point can be observe for different Al concentration and found to be decreasing with increasing of Al concentration.

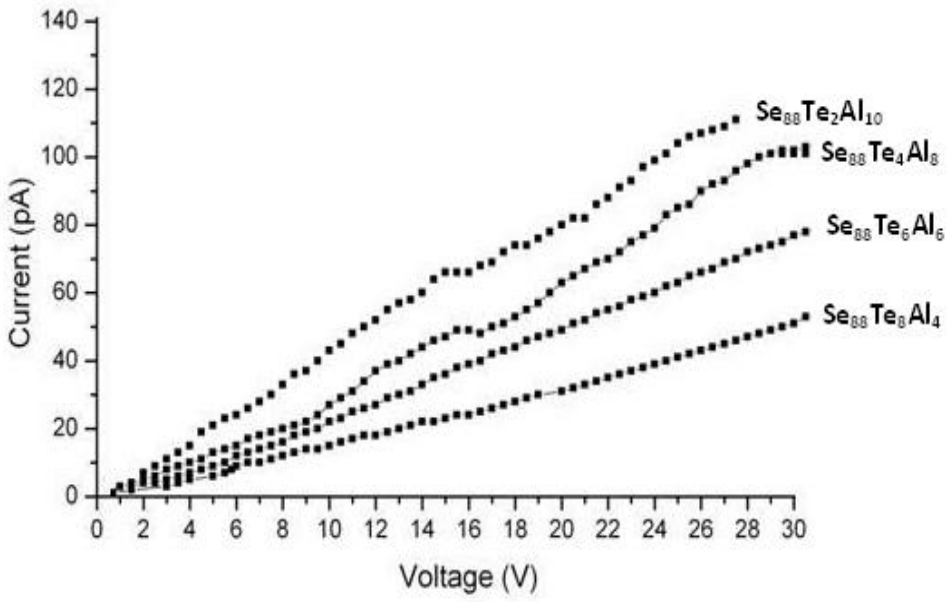

Figure 4.9: I-V graph of $Se_{88}Te_{12-x}Al_x$ at room temperature

Resistivity reduced with Al doping provided Al doping effectively improved $Se_{88}Te_{12-x}Al_x$ thin film electrical properties. Increase in σ_{dc} and σ_{ph} with the increasing Al concentration is expected when the density of the defect states is increasing in composition [48-50].

Temperature dependent steady state photoconductivity curve in $Se_{88}Te_{12-x}Al_x$ shows that the photoconductivity (σ_{ph}) increases exponentially with the temperature which indicates the existence of a single activation energy process in the observed temperature range. Normally, such dependence in chalcogenide glasses occurs in bimolecular recombination at the low-temperature end. The activation energies of photocurrents are smaller than dark thermal activation energy. This means that charge hopping in the photoexcitation takes place between the valence band and light-induced metastable defect states in the vicinity of the Fermi level. The differences in activation energies of dark current and photocurrent suggest that the photoexcitation takes place either from the localized states in the valence band tail or from impurity levels close to the valence band to the D centers. Thermally activated conduction is a common feature of chalcogenide glasses due to their semiconducting nature. In presence of light, the Fermi level splits into quasi Fermi levels and move towards the valence band for

holes and towards the conduction band for electrons. The position of these quasi Fermi levels depends on light intensity [14]. The activation energy therefore becomes smaller in the presence of light as compared to in dark. The value of γ has been evaluated which determines the type of recombination mechanism occurring in the system. The excess electrons and holes can either recombine among themselves or recombine with the charged centers. The former leads to a bimolecular recombination (BMR) and the latter to monomolecular recombination (MMR) [51, 52]. The value of γ for BMR and MMR are 0.5 and 1.0, respectively. It is found that γ varies from 0.62 to 0.66 in $Se_{88}Te_{12-x}Al_x$ system indicating that it is still in the transition region between the two recombination regimes. It indicates presence of localized or traps states in the gap of the material [22]. The rate of recombination is governed by the photo-generated carriers. Analysis shows that photosensitivity decreases with Al content which might be due to increase in density of localized states. Since, photosensitivity depends upon the lifetime of excess carriers which in, turns depends upon the density of localized states in a particular material. Higher the density of localized states will lower the lifetime and photosensitivity will therefore decrease. Since the persistent photoconductivity increases with Al concentration, it is expected that the persistent photoconductivity may be due to structural defects produce by addition of Al. In the case of non-exponential decay, differential lifetime (τ_d) is time dependent. The value of τ_d is found to be increase with increasing Al content, indicating the slower rate of decay. It might be due to Addition of Al gives rise to defect centers. These defects might induce more localized states which might act as trapping centers. Because of the involvement of electron and hole traps in the recombination process, additional processes of trap filling during the rise and trap emptying during the decay get involved. When sample subjected to light illumination, certain proportion of generated free carriers is captured by traps. The traps filled during excitation will be emptied after the cessation of illumination depending upon their capture cross-section and energy depth [53]. Slope of decay curve goes on decreasing as the decay time increases. This shows that the traps exist at all the energies in the band gap. These traps store the charge carrier and hence delay the recombination rate corresponding to the increase in the differential lifetime with the increase in the Al content. In this situation the recombination time is effectively dominated by the rate of trap emptying and is much greater than the carrier lifetime (τ_c) [54-57] as observed in present system

Conductivity measurement show that dark conductivity and photo conductivity increased with Al%. I-V graph confirm that increase in conductivity is due to increase in metallic additive Al which indicates increment of density of the defect states due to addition of Al content. Temperature dependent dark and photo conductivity shows the existence of a single activation energy process in the observed temperature range which indicates bimolecular charge carrier recombination. It is observed that d.c. and photo activation energies decreases with increasing Al content. The value of γ found from 0.62 to 0.66 which shows presence of localized or traps states in the gap of the material. Decrease in photosensitivity and increase in PPC with

increasing in Al content also shows structural defect production due to addition of Al content. Analysis of transient photoconductivity shows that τ_d increases with increasing Al content. It might be due to addition of Al gives rise to defect centers which induce more localized states to act as trapping centers. Slope of decay curve shows that the traps exist at all the energies in the band gap and hence delay the recombination rate. Carrier lifetime (τ_c) also found to be increasing with Al content. Photosensitivity study shows that it decreases with Al content which confirms that addition of Al content induce higher density of localized states.

4.6.1 Photo-induced Effect on $Se_{96-x}Te_4Hg_x$ Thin Films.

The temperature dependence of the dark current and the photocurrent have been studied in glassy $Se_{96-x}Te_4Hg_x$ (X = 4, 8 and 12) thin films in the temperature range 298 K- 373 K. The conductivity has been measured as a function of temperature at a constant voltage of 3V for all samples using equation 4.1. Taking results of these measurements $\ln(\sigma_{dc})$ versus 1000/T have been plotted and shown in Figure 4.10. Plot of temperature dependence of dark conductivity $\ln(\sigma_{dc})$ for $Se_{88}Te_{12-x}Al_x$ thin films found linear, indicating that the conduction is through an activated process having single activation energy. Therefore, σ_{dc} can be expressed by Arrhenius relation as given in equation 4.5. The value of d c activation energy

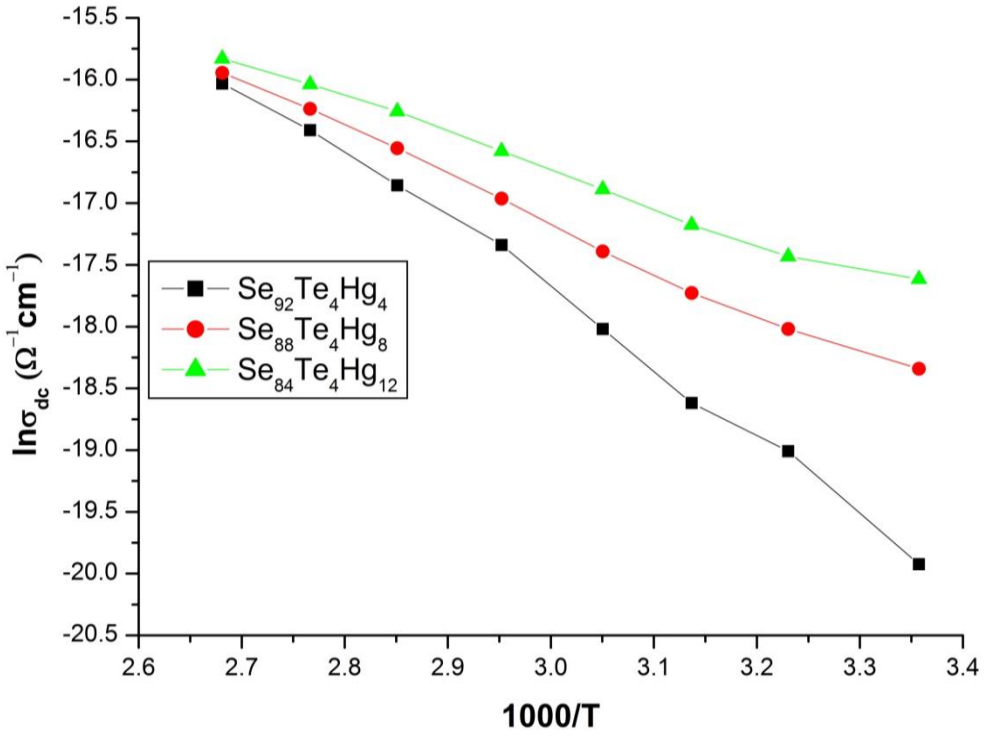

Figure 4.10: Temperature dependence of dark conductivity for various samples in a - $Se_{96-x}Te_4Hg_x$ thin films.

(ΔE_{dc}) has been estimated from the slope of $\ln(\sigma_{dc})$ versus 1000/T curves. The calculated value of σ_{dc}, ΔE_{dc} and σ_0 at 298K and given in table 4.2. From result it is observed that σ_{dc} and σ_0 increases with Hg concentration in $Se_{96-x}Te_4Hg_x$ glassy alloy. ΔE_{dc} found to be decrease with Al concentration. Decrease in the activation energy might be due to addition of more metallic impurities [21].

Temperature dependence of steady state photoconductivity has been studied in $Se_{88}Te_{12-x}Al_x$ system. It is found that $\sigma_{ph} > \sigma_{dc}$ in all sample and σ_{ph} also increases with Hg content. $\ln\sigma_{ph}$ versus 1000/T has been plotted and shown in figure 4.11.

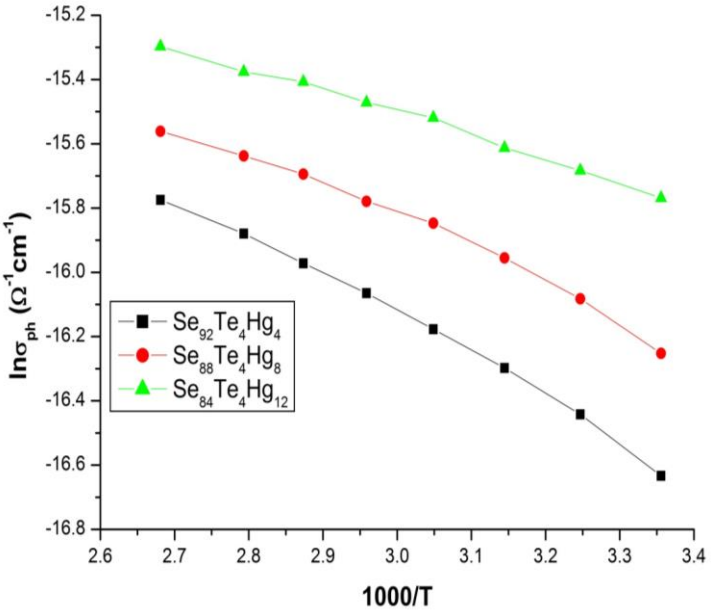

Figure 4.11: Temperature dependence of photoconductivity for various samples in a - $Se_{96-x}Te_4Hg_x$ thin films

Temperature dependent conductivity plot shows linear curve indicating that the photoconductivity is an activated process. The activation energy for photoconduction (ΔE_{ph}) is calculated from the slopes of $\ln\sigma_{ph}$ versus 1000/T curves and the values are given in table 4.2. It is observed that ΔE_{ph} decreases with increase in Hg%. The activation energy of photoconduction is much smaller than the activation energy in the dark. The well-defined activation energies suggest that the recombination centers are located at relatively discrete levels of localized states [21].

Steady state photoconductivity measurements as a function of light intensity (F) at room temperature shows that photoconductivity follows a power law with intensity [22, 23] according to equation 4.6 ($\sigma_{ph} \alpha F^{\gamma}$). The plot of $\ln\sigma_{ph}$ versus lnF for different Hg concentration found straight lines and has been shown in figure 4.12. The photoconductivity is found to be square-root-dependent on the light intensity. The power γ has been calculated

from the slopes of $\ln\sigma_{ph}$ versus lnF curves and is given in table 4.2. For all the compositions of $Se_{96-x}Te_4Hg_x$, γ is found near to 0.5 as given which confirms a bimolecular recombination mechanism in the studied films. And thus, indicating the presence of localized or traps states in the gap of the material [22].

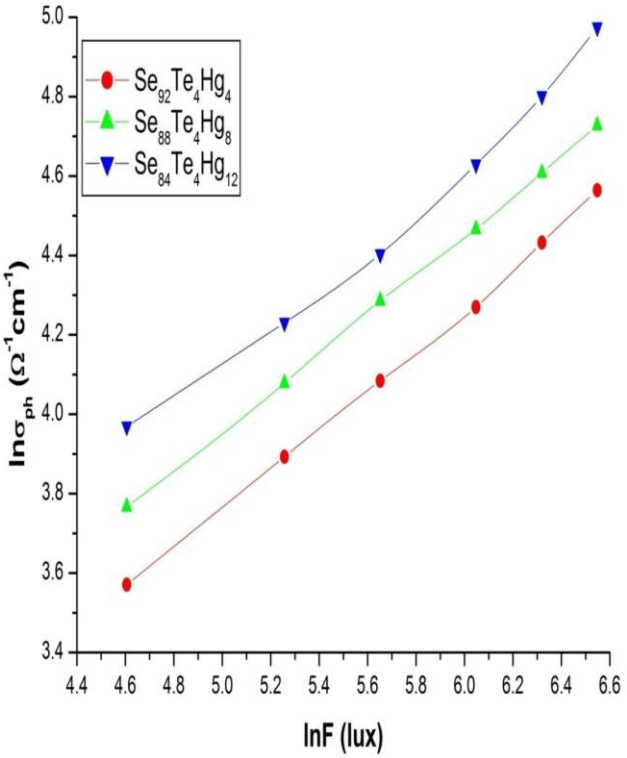

Figure 4.12: Variation of photoconductivity as a function of light intensity in a - $Se_{96-x}Te_4Hg_x$ thin films

Table 4.2: Various conductivity parameters at room temperature

Sample / Parameter	$Se_{92}Te_4Hg_4$	$Se_{88}Te_4Hg_8$	$Se_{84}Te_4Hg_{12}$
σ_{dc} $(\Omega^{-1}cm^{-1})$	2.2 X 10^{-9}	1.1 X 10^{-8}	2.2 X 10^{-8}
ΔE_{dc} (eV)	0.49	0.32	0.25
σ_0 $(\Omega^{-1}cm^{-1})$	0.42	6.06	8.04
σ_{ph} $(\Omega^{-1}cm^{-1})$	5.7 X 10^{-8}	8.7 X 10^{-8}	1.42 X 10^{-7}
ΔE_{ph} (eV)	0.10	0.09	0.06
σ_{ph}/σ_{dc}	25.90	7.91	0.65

γ	0.51	0.49	0.51
τ_1 (S)	2.53	2.81	2.94
τ_2 (S)	3.25	3.54	3.89
τ_{eff} (S)	1.42	1.57	1.68

Photosensitivity (σ_{ph} /σ_{dc}) of any material depends on the density of defect states and an important parameter to decide its use in photoconductive applications. σ_{ph} /σ_{dc} values for different compositions have been calculated at 600 lux at room temperature and given in Table 4.2. It is observed that photosensitivity decreases rapidly with increasing Hg % which indicates increase in defect states due to Hg addition. These defects may act as recombination centers in presence of light and are converted by bond switching reactions to random pairs of charged defects, known as light induced metastable defects (LIMDs) [58-60]. The charged defects act as charge trapping centers and decrease the photocurrent. A similar effect of defect states on photocurrent is reported in Se-Te-In alloys [61].

Transient photoconductivity measurements have been measured at intensity of 600 lux at temperature on the sample. After turning on light rise in current with time has been noted. After a certain time of illumination, when steady state achieved, light has been turned off and decay of the photocurrent has been measured. The initial dark current has been subtracted to obtain transient photocurrent. The rise and decay of photocurrent with time for all compositions are shown in Figure 4.13.

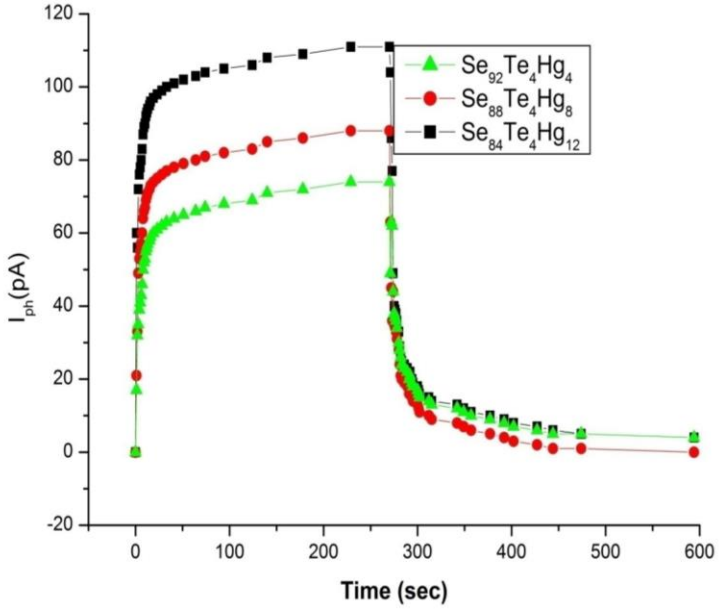

Figure 4.13: The rise and decay of photocurrent with time for all compositions

It is clear that the photocurrent initially rises fast then becomes slows, saturating after certain time. After get saturation current the light has been switched off and the photocurrent starts to decay quite fast initially, and then becomes slow. As time elapses it reaches steady state value as shown in figure 4.13. The decay process seems to be composed of two processes, a faster decay at the onset of transient and a slower decay later on. Any significant persistent photocurrent has not been observed in all compositions of $Se_{96-x}Te_4Hg_x$. The decay of photocurrent strongly depends on the characteristics of traps in a material. After light illumination, if the retrapping of carriers freed from traps is negligible then an exponential decay of photocurrent is expected provided the traps are monoenergetic [62] and can expressed as-

$$I_{ph}(t) = I_o \exp(-t/\tau) \qquad (4.9)$$

where $I_{ph}(t)$ is the value of the current at time t after the cessation of illumination and I_o corresponds to the photocurrent at t = 0. τ denotes the decay time constant and does not change with time like differential lifetime [63]. However, if there are traps of different kinds, then the resulting decay will be a sum of many exponential terms [62], each corresponding to a different set of traps and the plots of $\ln I_{ph}$ versus time will be a combination of different slopes. To analyze the experimental results the decay of photocurrent is plotted as shown in figure 4.14 on a semi-logarithmic scale with time.

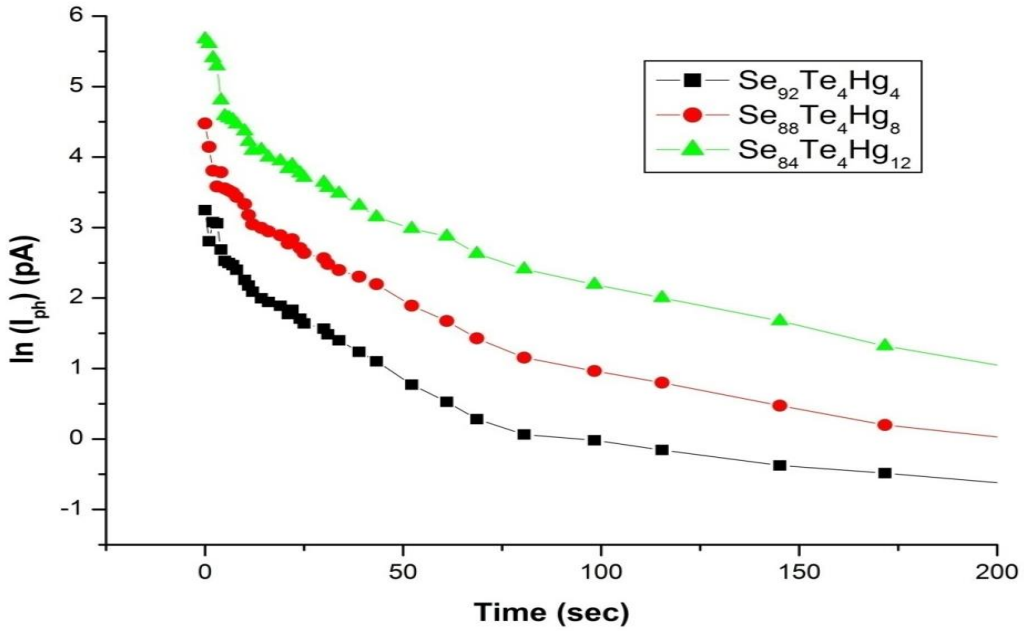

Figure 4.14: Decay of photocurrent ($\ln I_{ph}$) with time (t) for different Hg concentration at room temperature (298K) in $Se_{96-x}Te_4Hg_x$ thin film.

In present study, the decay of photocurrent is exponential and consists of two distinct parts, a fast component in the beginning and a slower decay afterwards, with different values of the decay time constants which can represent by the following relation-

$$I_{ph}(t) = I_1\exp(-t/\tau_1) + I_2\exp(-t/\tau_2) \quad (4.10)$$

Where I_1 and I_2 are the pre-exponential factors and τ_1 and τ_2 are the decay time constants for fast and slow parts respectively. Decay time constants τ_1 and τ_2 for faster and slower components have been calculated from the slopes of the decay curves and given in table 4.2. Decay of a similar nature has been reported in number of alloys [64,65]. Shallow traps give rise to fast component and deep traps were said to be responsible for the slower part of the decay. In order to have a rational comparison of the decay time constants, the concept of effective decay constant can be use [66]. In case of two processes with different decay time constants τ_1 and τ_2 participating in a mechanism simultaneously, then the effective time constant is given as

$$1/\tau_{eff} = 1/\tau_1 + 1/\tau_2 \quad (4.11)$$

The values of decay time constants for various compositions have been calculated and given in table 4.2. τ_{eff} values indicate that the decay of photocurrent gets slower with increasing Hg%, which indicates increment in the density of localized states in the mobility gap of Se-Te-Hg alloy. τ_1 and τ_2 shows a strong composition dependence and increases with increasing Hg content. τ_{eff} has composition dependence similar to that of τ_1 and τ_2 indicates that the resulting recombination is mainly due to carriers trapped. As can be seen from photosensitivity study which shows increment in localized defect energy states, which is in good agreement with τ_{eff} values. Also Increase in σ_{dc} and σ_{ph} with the increasing Hg concentration indicates that density of the defect states is increasing.

The effect of Hg content on the photoconductivity of $Se_{96-x}Te_4Hg_x$ thin film has been studied. Temperature dependence of steady state photocurrent reveals that photoconduction is an activated process and ΔE_{ph} decreases with increasing Hg concentration. The intensity dependence of photocurrent follows power law of photocurrent on incident radiation. Value of γ found to be approx 0.5 for all samples which confirms that recombination process takes place in present glassy system is bimolecular. It is found that $I_{ph} > I_{dc}$ in all samples at room temperature. Intensity dependence of decay photocurrent for all compositions is exponential and consists of two parts; one is fast decaying part and other is slow decaying. The concept of effective decay time constant (τ_{eff}) has been used to analyze the decay of photocurrent. Composition dependence of σ_{ph}/σ_{dc} and τ_{eff} confirms an increment in density of localized states in the energy gap with increasing Hg content.

4.7 References

[1] Willoughby Smith "Effect of Light on Selenium during the passage of an Electric current", Nature, 20 February 1873, p.303.

[2] RH Bube "Photoconductivity of Solids" Krieger Publ.Co, New York (1978)

[3] R.H.Bube "PllOtoeiectronic properties of semiconductors" Cambridge UniversityPress (1992)

[4] J. Mort and D.M Pai Photoconductivity and related phenomena" Elsevier, New York (1976)

[5] K.Weiser, RFisher and M.H Brodsky. "Proc. of the 10th into semiconductors Con! Cambridge U.S, AEC, Oak Ridge (1970)

[6] E.A Fagen and H.Fritzsche 1.Non-Cryst Solids 4 (1970) 480

[7] Simmons and O.W Taylor 1.Non-Cryst Solids 8-10, (1972) 947

[8] J.O Simmons and G.W Taylor 1.Plzys. C6, (1973) 3706

[9] G.W Taylor and J.O Simmons l.Phys C7 (1974) 3067

[10] T.C Arnoldussen, RH Bube, E.A Fagen and S.Holmberg 1.Non-Cryst Solids 8-10 (1972) 933

[11] Ivan Banik, Acta Electrotechnica et Informatica, Vol. 10, No. 3, 2010, 52–58

[12] H. Hamanaka, K. Tanaka, and S. Iizima, .Reversible photostructural change in melt-quenched As2S3 glass,. Solid State Commun. **23**, 63 (1977).

[13] Z. U. Borisova, Glassy Semiconductors (Plenum Press, New York,1981)

[14] M. Kastner, .Bonding bands, lone-pair bands, and impurity states in chalcogenide semiconductors,. Phys. Rev. Lett. **28** (6), 355 (1972).

[15] G. A. N. Connell, .Optical properties of amorphous semiconductors,. In Amorphous Semiconductors, edited by M. H. Brodsky (Springer-Verlag, Berlin, 1985), Vol. 36, pp. 73.

[16] P. W. Anderson, .Absence of diffusion in certain random lattices, Phys. Rev. **109** (5), 1492 (1958).

[17] P. Nagels, .Electronic transport in amorphous semiconductors,. in Amorphous Semiconductors, edited by M. H. Brodsky (Springer- Verlag, Berlin, 1985), Vol. 36, pp. 113.

[18] S. K. Tripathi and A. Kumar; J. Non-Cryst. Solids 104 (1988) 229.

[19] H. H. Weider, "Laboratory notes on electrical and galvanomagnetic measurements" EIsevier Scientific Publishing Company New York (1979)

[20] Mary R. Matthews, Robert J. Steed, Mark D. Frogley, and Chris C. Phillips, Applied Physics Letters **90**, (2007) 103519

[21] S. Singh, r. S. Sharma, r. K. Shukla, a. Kumar; steady state photoconductivity in a-$Se_{90}Ge_{10-x}In_x$ thin films; journal of optoelectronics and advanced materials vol. 6, no. 3, september 2004, p. 769 – 776.

[22] A. Rose, Concepts in Photoconductivity, Inter science, New York, 1963.

[23] R.H. Bube, Photoconductivity of Solids, Wiley, New York, 1960

[24] I. Watanable and T. Sekiya, Jpn. J. Appl. Phys., 28, 638 (1989).

[25] M. S. Kamboj, G. Kaur and R. Thangaraj, Thin Solid Films, 420-421, 350 (2002).

[26] A. Kumar, R. Misra and S. K. Tripathi, Semicod. Sci. Technol,. 4, 1151 (1989).

[27] M. Dixit, S. K. Dwivedi and A. Kumar, Thin Solid Films, 333, 165 (1998).

[28] D. V. Harea, I. A. Vasilev, E. P. Colomeico and M. S. Iovu, J. Optoelectronics and Advanced Materials, 5, 1115 (2003).

[29] W. Fuhs and D. Meyer, Phys. Stat. Sol. (a), 24, 274 (1974).

[30] K. Shimakawa, Y. Yano and Y. Katsuma, Philos. Mag. B, 54, 285 (1986).

[31] J. M. Chamberlain and A. J. Moseley, Jpn. J. Appl. Phys., 21, 13 (1982).

[32] M. Kumeda, G. Kawachi and T. Shimizu, Philos. Mag. B, 51, (5911985).
[33] S. K. Tripathi and A. Kumar, J Non { Cryst. Sol., 104, 229 (1988).
[34] S. Goel and A. Kumar, Thin Solid Films, 151, 307 (1987).
[35] A. M. Andriesh, in: \Physics and Applications of Non-Crystalline Semiconductors in Optoelectronics", Ed. A. M. Andriesh and M. Bertolotti, NATO ASI Series, 3. High Technologies Kluwer Acad. Publ., 36, 17 (1997),.
[36] M. S. Lovu, S. D. Shutov, L. Toth, Phys. Stat. Sol. (b), 195, 149 (1996).
[37] R. M. Mehra, G. Kaur and P. C. Mathur, Sol. Stat. Commun., 85, 29(1993).
[38] Choocho Lee and Byueng-Su yoo, Chinese J. Phys., 28, 93 (1990).
[39] J. F. Federici and D. M. Bubb, J. Superconductivity: Incoporating Novel Magnetism, 14, 331 (2001).
[40] Yeong-Ah Soh, G. Aeppli, F. M. Zimmermann, G. D. Isaacs, A. I. Frenkel, J. Appl. Phys., 90, 6172 (2001).
[41] W. Wang, S. J. Chua and G. Li, J. Electronic Materials, 29, (2000) 27
[42] D. Kumar, S. Kumar; Composition Dependence Of Photoconductivity In Amorphous Thin Films of Se:80−xTe:20Gex Turk J Phys, 29 (2005) , 91 - 96.
[43] R. K. Pal, A. K. Agnihotri, A. Kumar; Persistence Of Photoconductivity In Amorphous Se-Te-Zn System Chalcogenide Letters Vol. 7, No. 6, June 2010, P. 439-447.
[44] R. S. Sharma1, D. Kumar2, A. Kumar; Transient Photoconductivity In Amorphous Se-Ge-Ag System; Turk J Phys 30 (2006) , 47 – 55.
[45] W. Fuhs And D. Meyer, Phys. Status Solidi A 24, 295 (1974)
[46] I. Banik, Journal Of Optoelectronics And Advanced Materials, Vol. 11, No. 12, December 2009, P. 1931 - 1945
[47] S.S. Shariffudin, M. N. Masri, Abdul Aziz A,1M. F. Malek, M. Rusop, Photoresponse Characteristics of Aluminum Doped Zinc Oxide Thin Film ICSE2010 Proc. 2010, Melaka, Malaysia.
[48] J. C. Phillips, J. Non - Cryst. Solids, 43, (1981), 37.
[49] A. M. Ahmed, N. M. Megahid and M. M. Ibrahiem, Ind. J. Pure & Appl. Phys, 41, (2003), 863.
[50] S. Singh, R. S. Sharma,R. K. Shukla and A. Kumar, Vacuum, 72, (2004),1
[51] F.T. Reis, I. Chambouleyron: J. Non-Cryst. Solids 299–302, 179 (2002)
[52] N. Qamhieh, G.J. Adriaenssens: J. Non-Cryst. Solids 292, 80 (2001)
[53] A. S. MAAN, D. R. GOYAL; OPTOELECTRONICS AND ADVANCED MATERIALS – RAPID COMMUNICATIONS Vol. 1, No. 9, September 2007, p. 430 – 435
[54] R.M. Mehra, G. Kaur, P.C. Mathur, Solid State Commun. 85(1993) 29.
[55] W. Fuths, D. Meyer, Phys. Status Solidi a 24 (1974) 275.
[56] A.S. Mann, A.K. Sharma, D.R. Goyal, A. Kumar, J. Non-Cryst. Solids 104 (1988) 273.
[57] S. Jain, S. Gautam, D.K. Shukla, N. Goyal, Appl. Surf. Sci.147 (1999) 19.
[58] C. Main, A. E. Owen, Electronic and Structural Properties of amorphous semiconductors (Academic Press, London and New York, 1973).
[59] K. Shimakawa, J. Non Cryst. Solids **77,** 1253 (1985).
[60] K. Shimakawa, A. V. Kolobov, S. R. Elliot, Adv. Phys. **44**, 475 (1995).
[61] V. Sharma, A. Thakur, N. Goyal, G. S. S. Saini, S. K. Tripathi, J. Optoelectron. Adv. Mater. **7**, 2103 (2005).
[62] R. H. Bube, Photoconductivity in Solids (John Wiley and Sons Inc, 1979).

[63] W. Fuhs, D. Meyer, Phys Stat Solidi (a), **24,** 275 (1974).
[64] J. R. Haynes, J. A. Hornbeck, Phys. Rev., **100** 606 (1955).
[65] A. S. Maan, D. R. Goyal, A. Kumar, J. Non Cryst. Solids, **110**, 1384 (1989).
[66] Aldert Vander Ziel, Solid State Physical Electronics, (Prentice Hall India, 1971) 119.